

Supporting Information for:

Field Cricket Genome Reveals the Footprint of Recent, Abrupt Adaptation in the Wild

Sonia Pascoal^{1†}, Judith E. Risse^{2,3†}, Xiao Zhang^{4†}, Mark Blaxter^{5,6}, Timothee Cezard⁵, Richard J. Challis⁵, Karim Gharbi^{5,7}, John Hunt^{8,9}, Sujai Kumar⁵, Emma Langan^{5,10}, Xuan Liu¹¹, Jack G. Rayner⁴, Michael G. Ritchie⁴, Basten L. Snoek^{12,13}, Urmi Trivedi⁵, Nathan W. Bailey^{4,14}

¹Department of Zoology, University of Cambridge, CB2 3EJ, United Kingdom.

²Bioinformatics, Department of Plant Sciences, Wageningen University & Research, 6708 PB Wageningen, The Netherlands.

³Animal Ecology, Netherlands Institute of Ecology, PO Box 50, 6700 AB Wageningen, The Netherlands.

⁴School of Biology, University of St Andrews, St Andrews, Fife KY16 9TH, United Kingdom.

⁵Edinburgh Genomics, University of Edinburgh, Edinburgh EH9 3JT, United Kingdom.

⁶Institute of Evolutionary Biology, University of Edinburgh, Edinburgh EH9 3JT, United Kingdom.

⁷Earlham Institute, Norwich Research Park, Norwich NR4 7UZ, United Kingdom.

⁸School of Science and Health and the Hawkesbury Institute for the Environment, Western Sydney University, Penrith, NSW 2751, Australia.

⁹Centre for Ecology and Conservation, University of Exeter, Cornwall Campus, Penryn TR10 9FE, United Kingdom.

¹⁰School of Environmental Sciences, University of East Anglia, Norwich Research Park, Norwich NR4 7UZ, United Kingdom.

¹¹Centre for Genomic Research, University of Liverpool, Liverpool L69 7ZB, United Kingdom.

¹²Theoretical Biology and Bioinformatics, Utrecht University, Padualaan 8, 3584 CH Utrecht, The Netherlands.

¹³Terrestrial Ecology, Netherlands Institute of Ecology, PO Box 50, 6700 AB Wageningen, The Netherlands.

¹⁴E-mail: nwb3@st-andrews.ac.uk

† Contributed equally

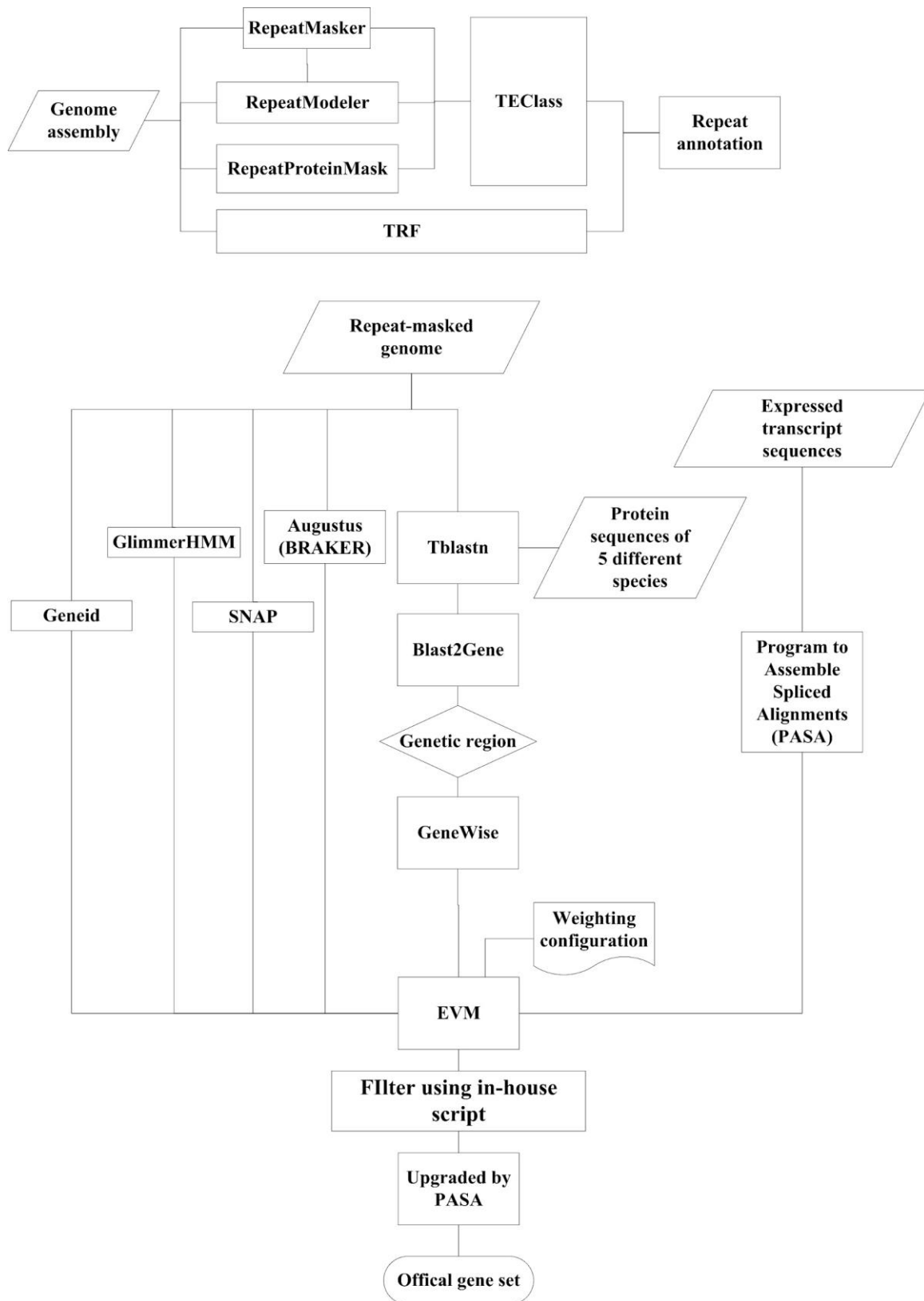


Figure S1. Workflow diagram of repeat annotation (top) and gene prediction (bottom) pipelines. Description of packages and parameters plus references are provided in the Methods section.

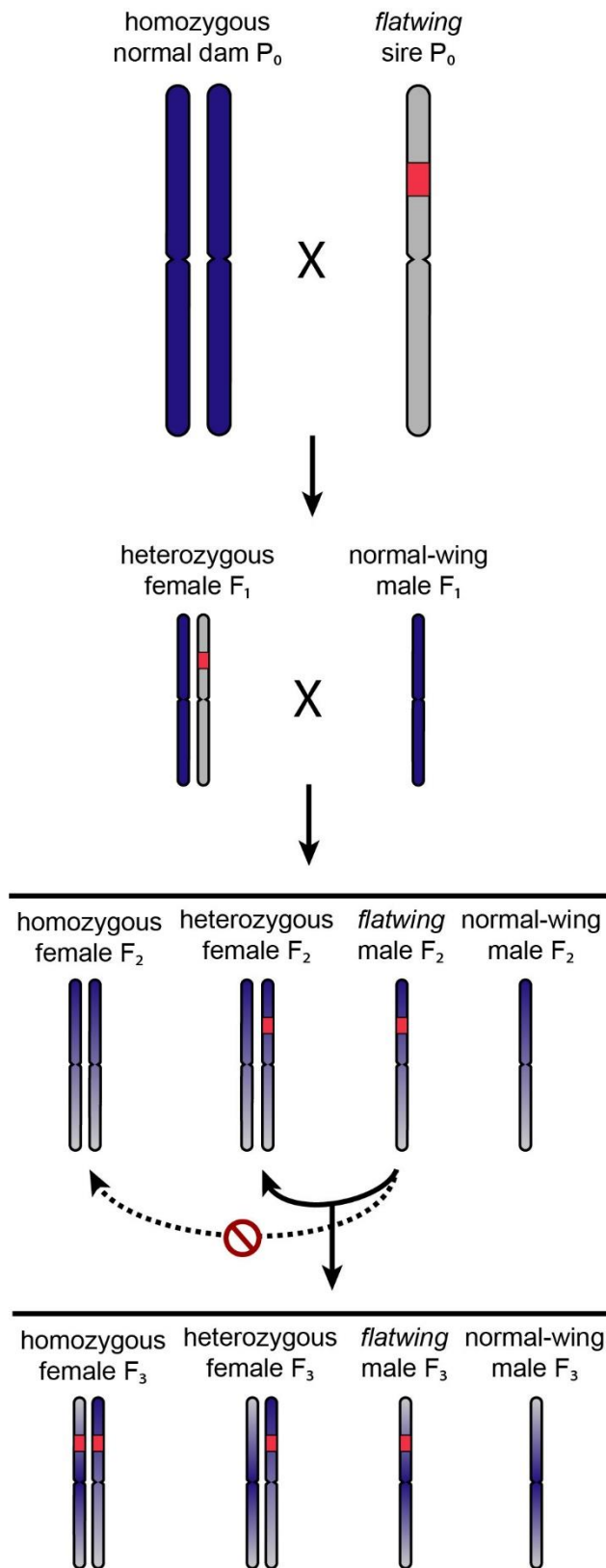


Figure S2. Cross design for linkage and QTL mapping. *Flatwing* segregates as a single-locus X-linked trait, so only X chromosomes are illustrated. A hypothetical *flatwing* locus is shaded in red. Females and males are XX/XO in *T. oceanicus*, so we performed three generations of crossing to enhance our ability to map *flatwing*. Homozygous *normal-wing* dams were obtained from a laboratory population of the same species originally derived from a population that has never contained *flatwing* (dark blue chromosomes). In the parental generation, these *normal-wing* dams were crossed to *flatwing* sires from Kauai (light grey chromosome, with hypothetical *flatwing* locus shaded in red). Dam genotypes were undetectable at generation F_2 due to *flatwing*'s sex-limited expression, so only full-sib crosses for which the *flatwing* male phenotype segregated in the subsequent F_3 generation were retained for phenotyping and QTL mapping (solid arrows).

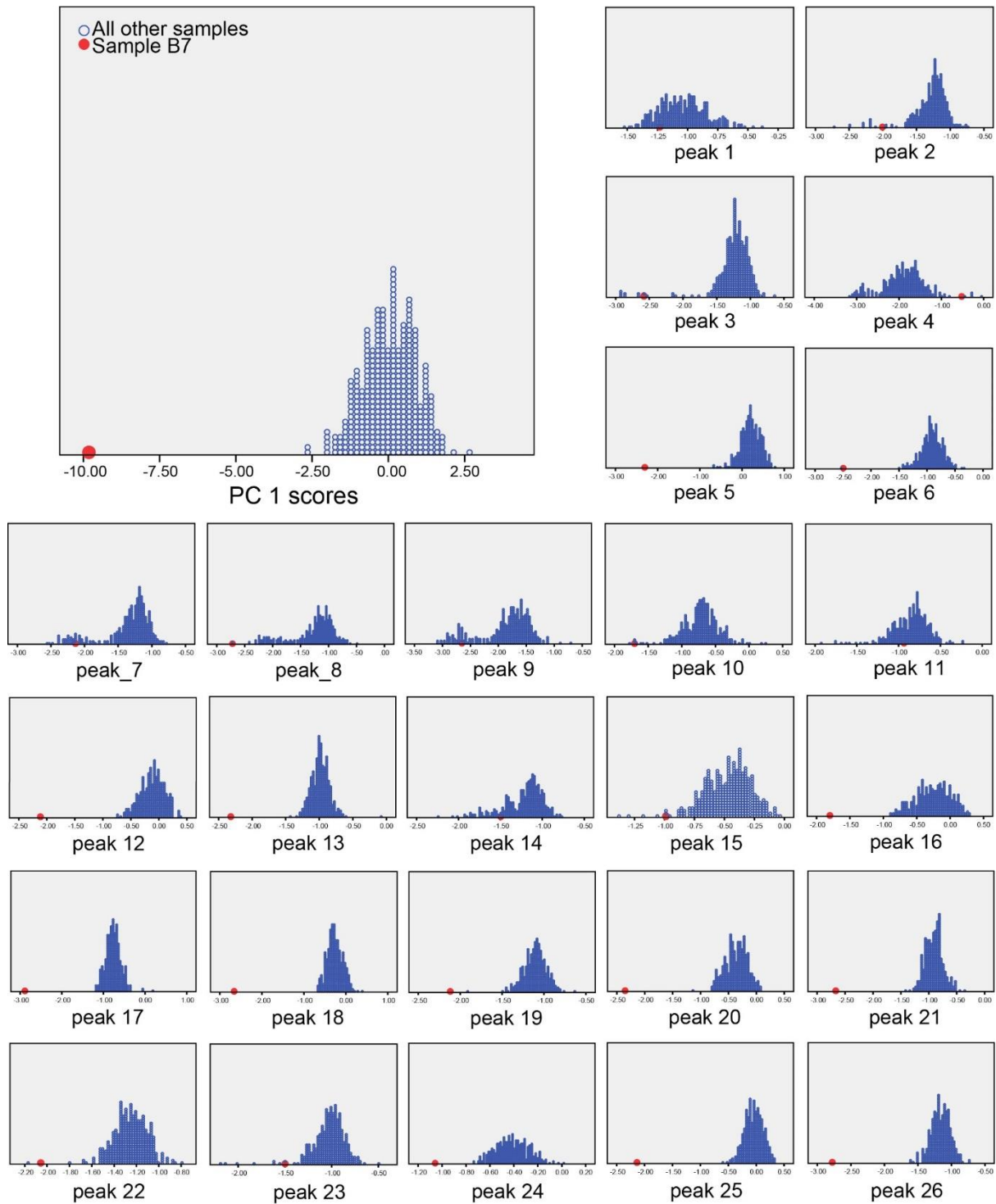


Figure S3. Histograms illustrating the identification of a CHC sample outlier. Sample B7, a normal-wing male, is indicated by the enlarged red dot in each plot. The sample was observed on visual inspection to deviate substantially from the distribution of principal component 1 scores for all other mapping individuals. Further inspection revealed this also to be the case in the majority of cases when the sample was assessed for each CHC peak individually. It was thus excluded from further analysis.

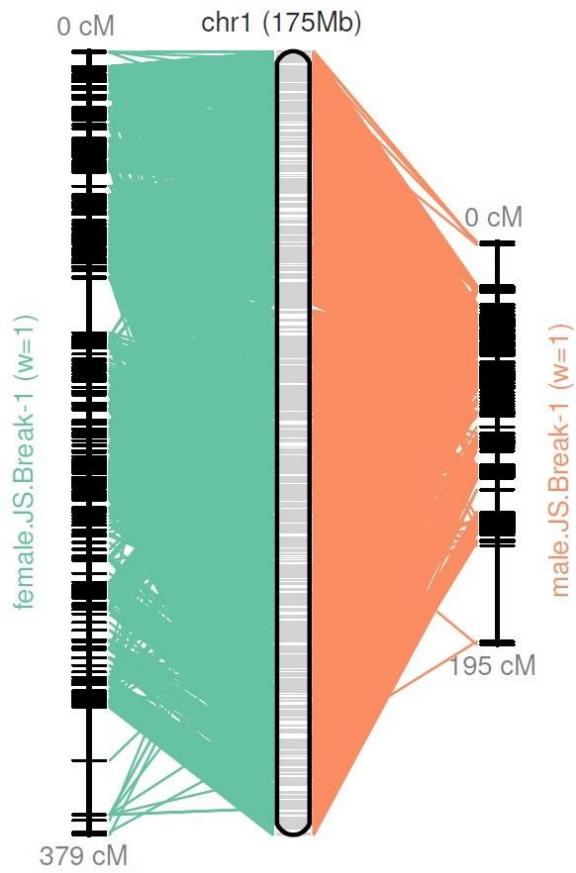


Figure S4. Reconstructed pseudomolecule for LG1 (putative X chromosome) using LOD5-supported markers. Lines connect the physical positions of markers on the pseudomolecule to female and male map positions (left and right, respectively).

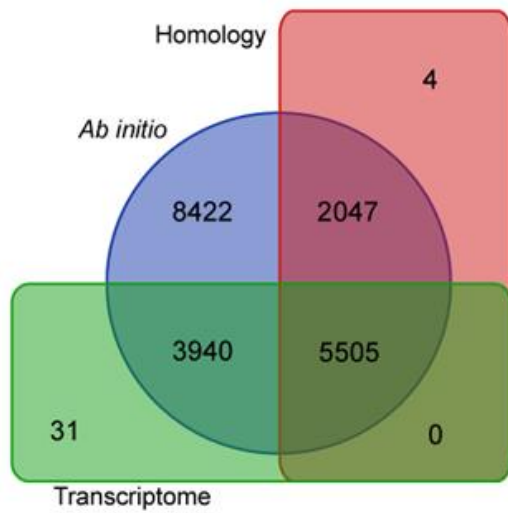


Figure S5. Venn diagram of genes predicted for *T. oceanicus* using different methods. Counts refer to the gene set that was obtained prior to final upgrade and filtering using PASA⁷³, so the total gene number above is slightly higher than the final gene set. A detailed description of each pipeline is presented in the Methods.

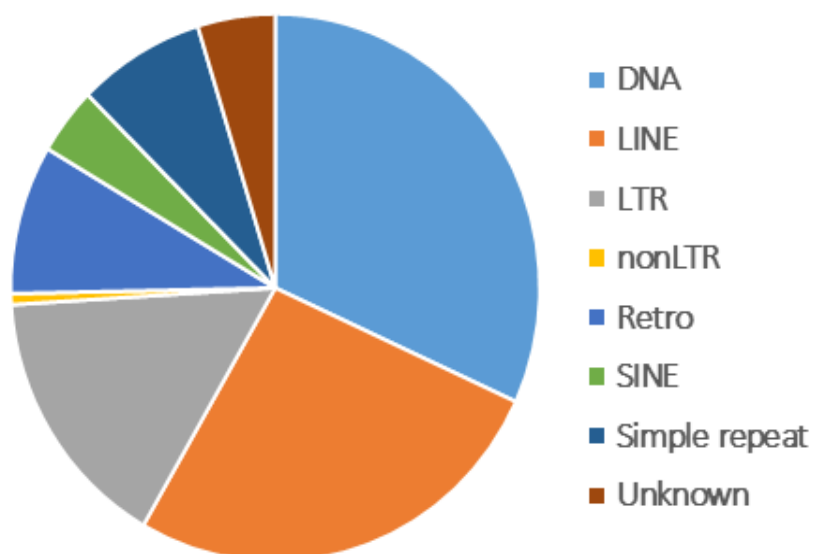


Figure S6. Proportions of eight major categories of transposable elements detected in the *T. oceanicus* genome.

DNA = DNA transposons

LTR = long terminal repeats

LINE = long interspersed nuclear elements

SINE = short interspersed nuclear elements

Retro = retrotransposon

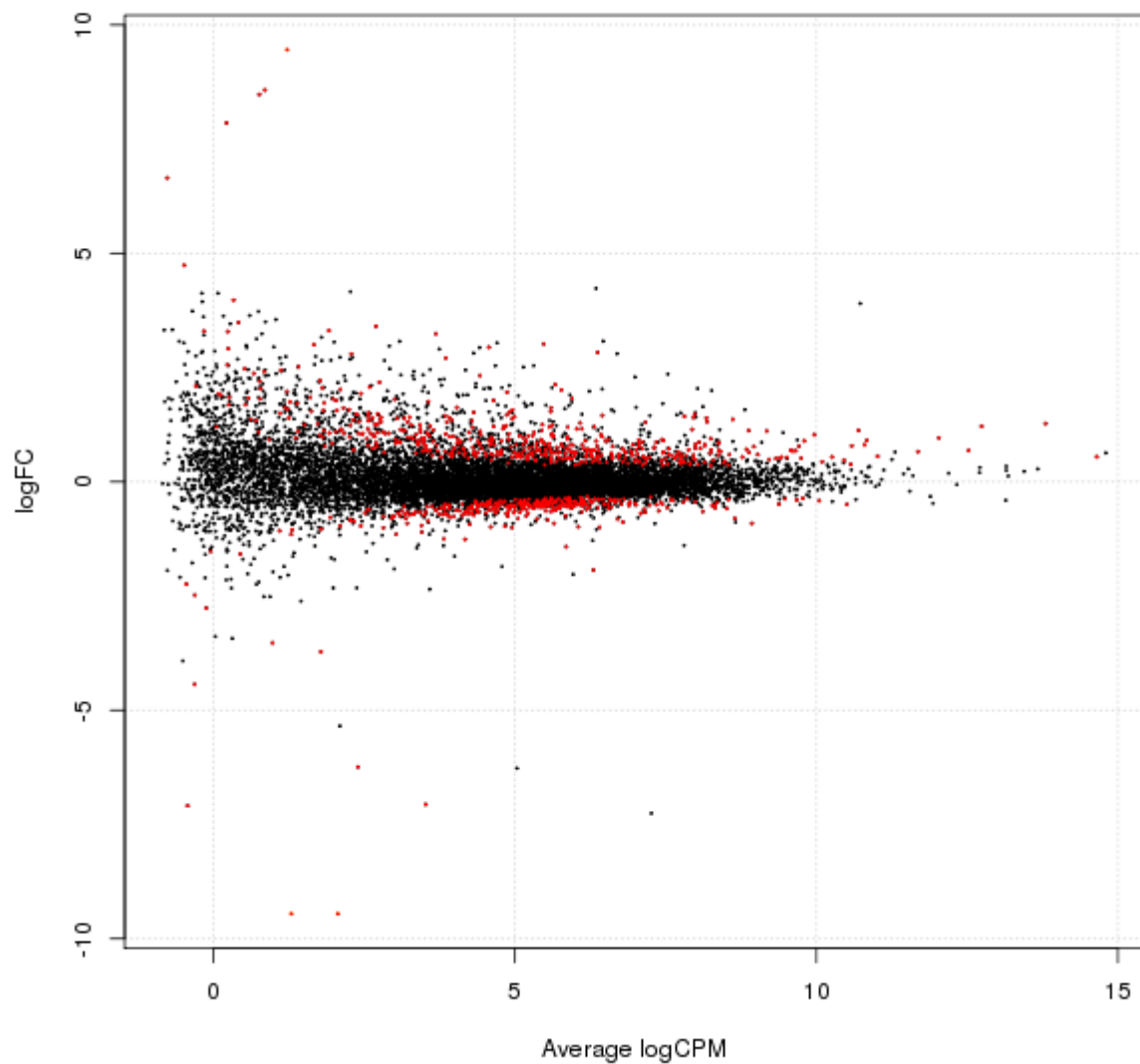


Figure S7. MA plot of thoracic genes DE between *T. oceanicus* embryos that were homozygous for *flatwing* vs. *normal-wing*. Red points indicate significantly differentially-expressed genes after filtering (see Methods), with positive values on the y-axis indicating genes downregulated in *flatwing* samples compared to *normal-wing* samples, and negative values indicating genes that are upregulated in *flatwing* samples. Log scales are base 2.

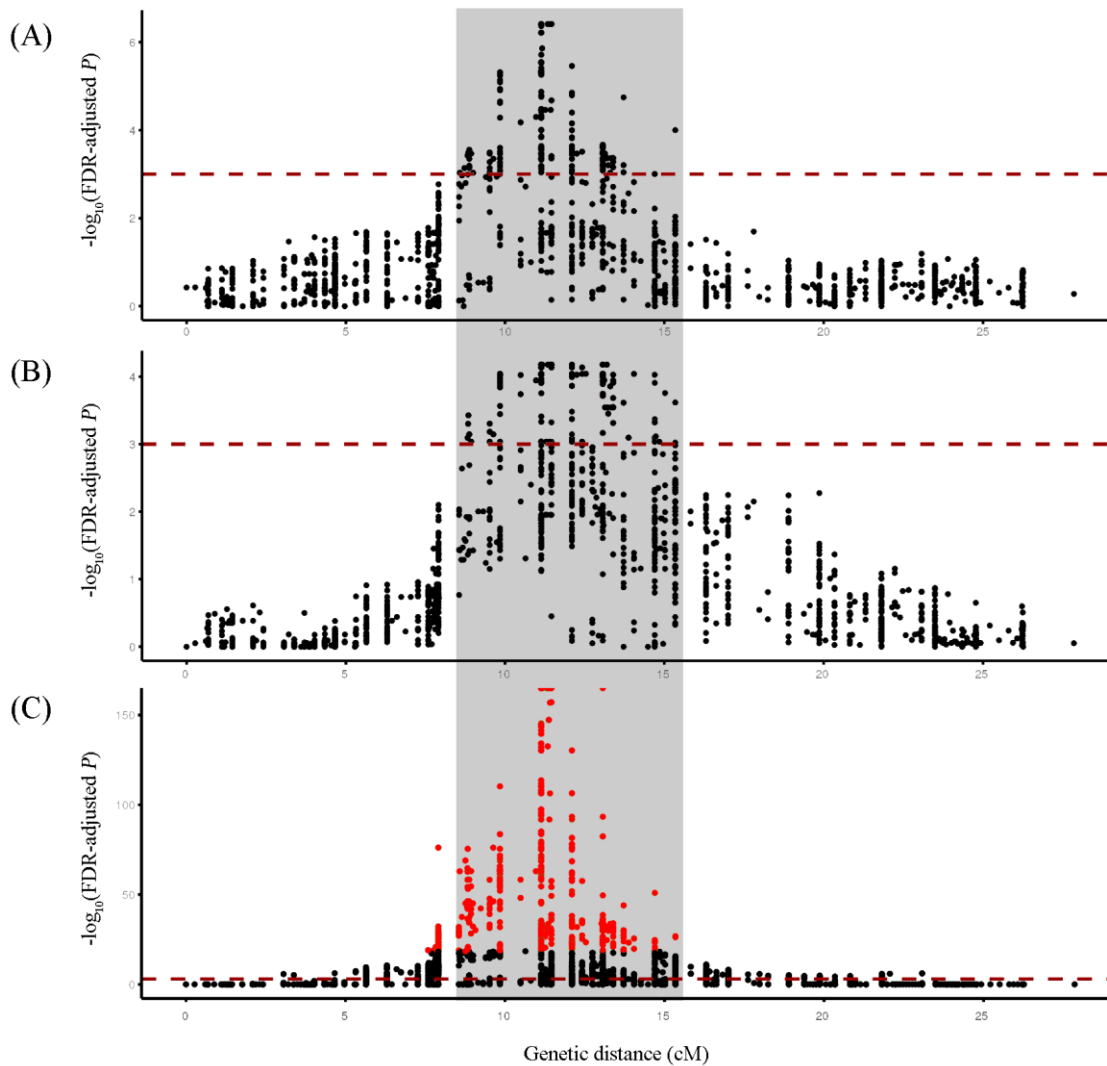


Figure S8. Genomic regions associated with different principal components describing male CHC profiles. Manhattan plot for LG1 (putative X chromosome) showing (A) the PC4-associated QTL, (B) PC6-associated QTL and (C) the *flatwing* QTL for comparison. The horizontal dashed lines indicate FDR-corrected significance threshold of $P < 0.001$, and the top 1% most significant flatwing-associated QTL markers are plotted in red in C. The light grey rectangle spans the genetic region in which flatwing-associated markers and CHC principal component-associated markers co-localize.

Table S1. Allele replacement table for identifying the X chromosome in the *T. oceanicus* linkage map

| Dam | Sire | Sire assumed | Sire rewrite | male current | male rewrite | male current | male rewrite |
|------------|-------------|---------------------|---------------------|---------------------|---------------------|---------------------|---------------------|
| 0/1 | 0/0 | 0/. | 0/2 | 0/0 | 0/2 | 1/1 | 1/2 |
| 0/1 | 1/1 | 1/. | 1/2 | 0/0 | 0/2 | 1/1 | 1/2 |
| 0/1 | 2/2 | 2/. | NA | - | - | - | - |
| 0/2 | 0/0 | 0/. | 0/1 | 0/0 | 0/1 | 2/2 | 1/2 |
| 0/2 | 1/1 | 1/. | NA | - | - | - | - |
| 0/2 | 2/2 | 2/. | 2/1 | 0/0 | 0/1 | 2/2 | 2/1 |
| 1/2 | 0/0 | 0/. | NA | - | - | - | - |
| 1/2 | 1/1 | 1/. | 1/3 | 1/1 | 1/3 | 2/2 | 2/3 |
| 1/2 | 2/2 | 2/. | 2/3 | 1/1 | 1/3 | 2/2 | 2/3 |

Table S2. Identification of *Teleogryllus oceanicus* cuticular hydrocarbon profile peaks using gas chromatography - mass spectrometry

| Peak ^a | Kováts retention index ^b | Identification | Diagnostic ions |
|-------------------|-------------------------------------|-------------------------|---|
| standard | | pentadecane | |
| 1 | 2840 | 4MeC ₂₈ | 365, 71 |
| 2 | 2893 | 10MeC ₂₈ | 281, 155 |
| 3 | 2910 | 13MeC ₂₉ | 252, 196 |
| 4 | 3028 | C _{30:1} | 434 |
| 5 | 3043 | 4MeC ₃₀ | 436, 393, 71 |
| 6 | 3064 | 7,x-diMeC ₃₀ | 365, 112 |
| 7 | 3075 | unidentified | |
| 8 | 3086 | C _{31:1} | 434 |
| 9 | 3110 | 11MeC ₃₁ | 308, 168 |
| 10 | 3119 | 7,8MeC ₃₁ | 364, 112 |
| 11 | 3130 | 7-C ₃₁ ene | 434, 528 ^c , 145 ^c , 383 ^c |
| 12 | 3142 | C _{31:1} | 434 |
| 13 | 3152 | C _{31:2} | 432 |
| 14 | 3161 | C _{31:2} | 432 |
| 15 | 3174 | C _{31:2} | 432 |
| 16 | 3188 | C _{31:2} | 432 |
| 17 | 3242 | 4MeC ₃₂ | 421, 71 |
| 18 | 3252 | unidentified | |
| 19 | 3268 | C _{32:2} | 446 |
| 20 | 3288 | C _{33:1} | 462 |
| 21 | 3331 | C _{33:1} | 462 |
| 22 | 3347 | C _{33:2} | 460 |
| 23 | 3355 | C _{33:2} | 460 |
| 24 | 3365 | C _{33:2} | 460 |
| 25 | 3379 | 3,x-C _{33:2} | 460, 647 ^c , 89 ^c |
| 26 | 3391 | C _{33:2} | 460 |

^a Peak identification is based on Table S4 of Pascoal et al. (2016) (Pascoal et al. 2016b), reproduced here.

The 26 quantified peaks are presented in sequential order in the table and in Fig. 3A of the main text.

^b Calculation of the Kováts retention index using *n*-alkane standards (C₇ - C₄₀) is described in Majlát et al. (1974) (Majlát et al. 1974)

^c Ions used when identifying with dimethyl-disulphide derivation

Table S3. *T. oceanicus* genome metrics

| | | |
|--|--------------------|------------------------------|
| Maximum scaffold length (bp) | 2,637,780 | |
| Complete BUSCO (Ref total = 1,066) | 1,001 | |
| % complete BUSCO (genome) | 93.9% | |
| % complete BUSCO (gene set) ^a | 83.2% | |
| Scaffold metrics | All contigs | Contigs > 1,000 bp |
| Total bases (gb) | 2,045,067,382 | 2,044,651,628 |
| N50 (bp) | 62,615 | 62,685 |
| Sequences in N50 | 6,139 | 6,136 |
| GC content (%) | 40 | 40 |
| Mean scaffold length (bp) | 10,335 | 10,355 |
| Sequencing library yields | Read pairs | Yield (GB) |
| Illumina TruSeq 180 | 277,076,641 | 55.42 |
| Illumina TruSeq 300 | 243,927,180 | 48.79 |
| Illumina TruSeq 600 | 238,275,727 | 47.66 |
| Illumina TruSeq Nano 350 | 70,959,741 | 14.19 |
| Illumina TruSeq Nano 550 | 63,415,263 | 12.68 |
| Illumina Nextera mate-pair | 229,431,023 | 45.89 |
| PacBio RSII | 5,771,779 | 21.74 |

^a Final gene number identified in Table S8

Table S4. List of chimeric scaffolds identified and corrected in the *T. oceanicus* genome

| Chimeric scaffold | Coordinates | | Corrected scaffold | Linkage group |
|--------------------|-------------|--------|----------------------|---------------|
| | Start | Stop | | |
| Contig112_pilon | 1 | 280481 | Contig112_pilon.1 | LG13 |
| Contig112_pilon | 285560 | 415702 | Contig112_pilon.2 | LG4 |
| Contig115174_pilon | 1 | 4504 | Contig115174_pilon.1 | LG3 |
| Contig115174_pilon | 4505 | 9682 | Contig115174_pilon.2 | LG5 |
| Contig11656_pilon | 1 | 69510 | Contig11656_pilon.1 | LG3 |
| Contig11656_pilon | 71880 | 189927 | Contig11656_pilon.2 | LG2 |
| Contig122717_pilon | 1 | 791 | Contig122717_pilon.1 | LG12 |
| Contig122717_pilon | 792 | 1738 | Contig122717_pilon.2 | LG13 |
| Contig12684_pilon | 1 | 94718 | Contig12684_pilon.1 | LG14 |
| Contig12684_pilon | 94719 | 233653 | Contig12684_pilon.2 | LG16 |
| Contig157093_pilon | 1 | 21374 | Contig157093_pilon.1 | LG1 |
| Contig157093_pilon | 21375 | 29205 | Contig157093_pilon.2 | LG2 |
| Contig16901_pilon | 1 | 14926 | Contig16901_pilon.1 | LG16 |
| Contig16901_pilon | 18394 | 186701 | Contig16901_pilon.2 | LG11 |
| Contig17374_pilon | 1 | 391141 | Contig17374_pilon.1 | LG11 |
| Contig17374_pilon | 392712 | 614243 | Contig17374_pilon.2 | LG3 |
| Contig19418_pilon | 1 | 216097 | Contig19418_pilon.1 | LG10 |
| Contig19418_pilon | 220070 | 446236 | Contig19418_pilon.2 | LG12 |
| Contig24478_pilon | 1 | 10308 | Contig24478_pilon.1 | LG19 |
| Contig24478_pilon | 13057 | 232760 | Contig24478_pilon.2 | LG13 |
| Contig25912_pilon | 1 | 178241 | Contig25912_pilon.1 | LG12 |
| Contig25912_pilon | 180760 | 432977 | Contig25912_pilon.2 | LG11 |
| Contig3004_pilon | 1 | 113166 | Contig3004_pilon.1 | LG10 |
| Contig3004_pilon | 113846 | 201707 | Contig3004_pilon.2 | LG1 |
| Contig30253_pilon | 1 | 75616 | Contig30253_pilon.1 | LG6 |
| Contig30253_pilon | 75924 | 107012 | Contig30253_pilon.2 | LG10 |
| Contig30890_pilon | 1 | 42473 | Contig30890_pilon.1 | LG7 |

| | | | | |
|-------------------|--------|--------|---------------------|------|
| Contig30890_pilon | 42474 | 357127 | Contig30890_pilon.2 | LG4 |
| Contig32501_pilon | 1 | 79400 | Contig32501_pilon.1 | LG8 |
| Contig32501_pilon | 81158 | 104315 | Contig32501_pilon.2 | LG5 |
| Contig34163_pilon | 1 | 276874 | Contig34163_pilon.1 | LG14 |
| Contig34163_pilon | 278116 | 477845 | Contig34163_pilon.2 | LG8 |
| Contig34793_pilon | 1 | 35174 | Contig34793_pilon.1 | LG13 |
| Contig34793_pilon | 35175 | 226445 | Contig34793_pilon.2 | LG4 |
| Contig37346_pilon | 1 | 181531 | Contig37346_pilon.1 | LG1 |
| Contig37346_pilon | 185444 | 510953 | Contig37346_pilon.2 | LG5 |
| Contig44873_pilon | 1 | 96939 | Contig44873_pilon.1 | LG3 |
| Contig44873_pilon | 100500 | 540225 | Contig44873_pilon.2 | LG2 |
| Contig53403_pilon | 1 | 162159 | Contig53403_pilon.1 | LG1 |
| Contig53403_pilon | 163594 | 231179 | Contig53403_pilon.2 | LG12 |
| Contig6264_pilon | 1 | 582129 | Contig6264_pilon.1 | LG1 |
| Contig6264_pilon | 582130 | 671930 | Contig6264_pilon.2 | LG16 |
| Contig6264_pilon | 675095 | 875693 | Contig6264_pilon.3 | LG1 |
| Contig67999_pilon | 1 | 75111 | Contig67999_pilon.1 | LG8 |
| Contig67999_pilon | 80918 | 230728 | Contig67999_pilon.2 | LG16 |
| Contig7355_pilon | 1 | 31398 | Contig7355_pilon.1 | LG4 |
| Contig7355_pilon | 31626 | 89218 | Contig7355_pilon.2 | LG7 |

Table S5. Summary statistics describing scaffold anchoring on *T. oceanicus* LOD5 linkage map markers

26
27

| | Anchored | Oriented | Unplaced |
|---------------------------------|------------------------|------------------------|--------------------------|
| Markers (unique) | 104,713 | 88,665 | 741 |
| Markers per Mb | 143.9 | 154.5 | 0.6 |
| Scaffolds | 8,169 | 5,997 | 189,726 |
| Scaffolds with 1 marker | 686 | 0 | 187 |
| Scaffolds with 2 markers | 587 | 471 | 63 |
| Scaffolds with 3 markers | 578 | 368 | 37 |
| Scaffolds with ≥ 4 markers | 6,318 | 5,158 | 50 |
| Total bases | 727,468,034 (35.6%) | 573,790,325 (28.1%) | 1,317,555,539 (64.4%) |

Table S6. Functional annotation of *T. oceanicus* genes

28
29

| | | Number | Proportion of all genes (%) |
|------------------|----------------|--------|-----------------------------|
| Total | | 19,157 | - |
| Annotated | InterPro | 12,318 | 64.3 |
| | Swissprot | 11,754 | 61.4 |
| | TrEMBL | 13,999 | 73.1 |
| | NR | 13,989 | 73.0 |
| | Gene Ontology | 13,177 | 68.7 |
| | KEGG | 9,579 | 50.0 |
| | All annotated | 14,367 | 75.0 |
| | Unknown | | 4,790 |

Table S7. Distribution of repetitive elements for each scaffolded *T. oceanicus* linkage group

| Linkage group | Transposable elements (kb) | % | Rank ^a | Tandem repeats (kb) | % | Rank ^a | Combined (kb) | % | Rank ^a |
|---------------|----------------------------|------|-------------------|---------------------|-----|-------------------|---------------|------|-------------------|
| LG1 | 65992 | 38.6 | 8 | 1832 | 1.1 | 20 | 67823 | 39.7 | 11 |
| LG2 | 26518 | 35.7 | 17 | 1123 | 1.5 | 14 | 27641 | 37.2 | 17 |
| LG3 | 12908 | 36.3 | 14 | 572 | 1.6 | 13 | 13480 | 37.9 | 14 |
| LG4 | 16514 | 42.0 | 2 | 848 | 2.2 | 4 | 17362 | 44.2 | 2 |
| LG5 | 10253 | 36.2 | 15 | 500 | 1.8 | 11 | 10753 | 37.9 | 15 |
| LG6 | 23187 | 35.0 | 18 | 925 | 1.4 | 17 | 24113 | 36.4 | 18 |
| LG7 | 17533 | 36.3 | 13 | 936 | 1.9 | 8 | 18469 | 38.2 | 13 |
| LG8 | 12770 | 38.8 | 6 | 617 | 1.9 | 7 | 13387 | 40.7 | 6 |
| LG9 | 9952 | 38.2 | 9 | 659 | 2.5 | 2 | 10611 | 40.7 | 7 |
| LG10 | 9359 | 38.2 | 10 | 545 | 2.2 | 5 | 9904 | 40.5 | 8 |
| LG11 | 18920 | 34.1 | 19 | 804 | 1.5 | 15 | 19724 | 35.6 | 19 |
| LG12 | 4850 | 42.7 | 1 | 297 | 2.6 | 1 | 5148 | 45.4 | 1 |
| LG13 | 12684 | 37.4 | 12 | 624 | 1.8 | 10 | 13308 | 39.2 | 12 |
| LG14 | 12629 | 36.2 | 16 | 483 | 1.4 | 16 | 13112 | 37.6 | 16 |
| LG15 | 1298 | 41.7 | 3 | 53 | 1.7 | 12 | 1351 | 43.5 | 3 |
| LG16 | 6292 | 31.5 | 20 | 243 | 1.2 | 19 | 6535 | 32.7 | 20 |
| LG17 | 337 | 39.5 | 5 | 10 | 1.2 | 18 | 347 | 40.7 | 5 |
| LG18 | 699 | 38.2 | 11 | 42 | 2.3 | 3 | 741 | 40.5 | 9 |
| LG19 | 3 | 27.4 | 21 | 0 | 0.4 | 21 | 3 | 27.8 | 21 |
| Unplaced | 526597 | 40.0 | 4 | 25416 | 1.9 | 6 | 552013 | 41.9 | 4 |
| Total | 789295 | 38.6 | 7 | 36531 | 1.8 | 9 | 825826 | 40.4 | 10 |

^a Sorted by the proportion of repetitive elements in linkage groups, from most to fewest

Table S8. Comparison of gene features among ten insect species

| Species | Genome assembly size (Gb) | Gene number | Single exon gene number | % | Average gene length | Average CDS length (bp) | Average exon number per transcript | Average exon length (bp) | Ref. |
|---------------------------------|---------------------------|-------------|-------------------------|------|---------------------|-------------------------|------------------------------------|--------------------------|-------------------------------------|
| Field cricket | | | | | | | | | |
| <i>Teleogryllus oceanicus</i> | 2.0 | 19,157 | 1,266 | 6.6 | 12,232 | 1,184 | 6.2 | 395 | <i>this study</i> |
| Migratory locust | | | | | | | | | |
| <i>Locusta migratoria</i> | 6.5 | 17,307 | 3,079 | 17.8 | 54,341 ^a | 1,160 | 5.8 | 201 | (Wang et al. 2014) |
| American Cockroach | | | | | | | | | |
| <i>Periplaneta americana</i> | 3.4 | 21,336 | 2,704 | 12.7 | 12,963 ^b | - | 4 ^b | 247 ^b | (Li et al. 2018) |
| Fruit fly | | | | | | | | | |
| <i>Drosophila melanogaster</i> | 0.1 | 13,689 | 2,761 | 20.2 | 4,261 | 1,621 | 4.0 | 408 | (Gramates et al. 2017) ^c |
| Asian long-horned beetle | | | | | | | | | |
| <i>Anoplophora glabripennis</i> | 0.7 | 16,200 | 1,194 | 7.4 | 18,596 | 1,744 | 6.6 | 265 | (McKenna et al. 2016) |
| Bed bug | | | | | | | | | |
| <i>Cimex lectularius</i> | 0.7 | 13,751 | 1,410 | 10.3 | 29,076 | 1,846 | 10.2 | 265 | (Rosenfeld et al. 2016) |
| Brown planthopper | | | | | | | | | |
| <i>Nilaparvata lugens</i> | 1.1 | 21,442 | 2,179 | 10.2 | 22,015 | 1,440 | 6.9 | 289 | (Xue et al. 2014) |
| Dampwood termite | | | | | | | | | |
| <i>Zootermopsis nevadensis</i> | 0.5 | 15,129 | 370 | 2.4 | 24,927 | 1,890 | 9.4 | 365 | (Terrapon et al. 2014) |
| Yellow fever mosquito | | | | | | | | | |
| <i>Aedes aegypti</i> | 1.3 | 19,585 | 1,158 | 5.9 | 36,583 | 2,144 | 6.4 | 481 | (Dudchenko et al. 2017) |
| Asian Tiger mosquito | | | | | | | | | |
| <i>Aedes albopictus</i> | 2.2 | 38,706 | 2,305 | 6.0 | 25,506 | 1,950 | 5.3 | 440 | (Miller et al. 2018) |

^a Originally reported average transcript length^b Originally reported medians^c Adapted from (Wang et al. 2014)

Table S9. Transposable element classification in *T. oceanicus* contrasted with three published genomes

| Types | <i>T. oceanicus</i> | | <i>L. migratoria</i> ^a | | <i>D. melanogaster</i> ^a | | <i>H. sapiens</i> ^a | |
|---------------|---------------------|-------------|-----------------------------------|-------------|-------------------------------------|-------------|--------------------------------|-------------|
| | Repeat size (bp) | % of genome | Repeat size (bp) | % of genome | Repeat size (bp) | % of genome | Repeat size (bp) | % of genome |
| DNA | 259181458 | 12.7 | 1,480,538,225 | 22.7 | 4,849,763 | 2.9 | 99,797,428 | 3.2 |
| LINE | 215705991 | 10.5 | 1,332,720,207 | 20.4 | 12,119,904 | 7.2 | 637,919,432 | 20.3 |
| LTR | 127951980 | 6.3 | 508,675,263 | 7.8 | 21,849,378 | 13.0 | 267,738,295 | 8.5 |
| nonLTR | 5233875 | 0.3 | 63,892,419 | 1.0 | - | - | - | - |
| Retro | 71828043 | 3.5 | 153,548,453 | 2.4 | - | - | - | - |
| SINE | 32344731 | 1.6 | 141,176,698 | 2.2 | 52,841 | 0.0 | 397,225,496 | 12.7 |
| Simple repeat | 63555524 | 3.1 | 13,026,240 | 0.2 | 2,733 | 0.0 | 26,240,511 | 0.8 |
| Unknown | 38615245 | 1.9 | 406,097,360 | 6.2 | 11,211,970 | 6.6 | 1,298,163 | 0.0 |
| Total | 789295269 | 38.6 | 3,840,808,141 | 58.9 | 50,785,143 | 30.0 | 1,434,373,137 | 46.0 |

DNA = DNA transposons

LTR = long terminal repeats

LINE = long interspersed nuclear elements

SINE = short interspersed nuclear elements

Retro = retrotransposon

^a Data from (Wang et al. 2014)

Table S10. Thoracic gene expression variation between embryonic crickets carrying *flatwing* vs. *normal-wing* genotypes

| | |
|--|--------|
| Total number of genes passing expression filtering | 10,961 |
| Total DE genes | 830 |
| Up-regulated in <i>flatwing</i> | 328 |
| Down-regulated in <i>flatwing</i> | 502 |
| DE genes with $\log_2FC > 1$ | 204 |
| Up-regulated in <i>flatwing</i> | 25 |
| Down-regulated in <i>flatwing</i> | 179 |

Table S11. GO analysis of thoracic DEGs between embryos carrying *flatwing* vs. *normal-wing* genotypes

| GO | Type | Function | No. of DEGs | P-adj. |
|------------|--------------------|--|-------------|--------|
| GO:0003824 | molecular_function | catalytic activity | 216 | 0.006 |
| GO:0016787 | molecular_function | hydrolase activity | 80 | 0.027 |
| GO:0044087 | biological_process | regulation of cellular component biogenesis | 20 | 0.004 |
| GO:0051493 | biological_process | regulation of cytoskeleton organization | 12 | 0.023 |
| GO:0090066 | biological_process | regulation of anatomical structure size | 12 | 0.009 |
| GO:0097435 | biological_process | supramolecular fiber organization | 12 | 0.023 |
| GO:0032535 | biological_process | regulation of cellular component size | 11 | 0.004 |
| GO:0032956 | biological_process | regulation of actin cytoskeleton organization | 11 | 0.001 |
| GO:0032970 | biological_process | regulation of actin filament-based process | 11 | 0.001 |
| GO:1902903 | biological_process | regulation of supramolecular fiber organization | 11 | 0.002 |
| GO:0043254 | biological_process | regulation of protein complex assembly | 10 | 0.035 |
| GO:0110053 | biological_process | regulation of actin filament organization | 10 | 0.001 |
| GO:0008064 | biological_process | regulation of actin polymerization or depolymerization | 8 | 0.006 |
| GO:0030832 | biological_process | regulation of actin filament length | 8 | 0.006 |
| GO:0030833 | biological_process | regulation of actin filament polymerization | 8 | 0.006 |
| GO:0032271 | biological_process | regulation of protein polymerization | 8 | 0.015 |
| GO:0015630 | cellular_component | microtubule cytoskeleton | 6 | 0.001 |
| GO:0005248 | molecular_function | voltage-gated sodium channel activity | 5 | 0.004 |
| GO:0010927 | biological_process | cellular component assembly involved in morphogenesis | 5 | 0.010 |
| GO:0034706 | cellular_component | sodium channel complex | 4 | 0.007 |

Table S12. KEGG pathway enrichment of thoracic DEGs between embryos carrying *flatwing* vs. *normal-wing* genotypes

| ID^a | Pathway | No. of genes | P-value^b | P-adj.^c |
|-----------------------|---|---------------------|----------------------------|---------------------------|
| map04520 | Adherens junction | 13 | <0.001 | 0.025 |
| map03030 | DNA replication | 9 | 0.001 | 0.264 |
| map05100 | Bacterial invasion of epithelial cells | 9 | 0.007 | 0.408 |
| map05130 | Pathogenic Escherichia coli infection | 9 | 0.005 | 0.408 |
| map01100 | Metabolic pathways | 59 | 0.013 | 0.552 |
| map04960 | Aldosterone-regulated sodium reabsorption | 5 | 0.012 | 0.552 |
| map04064 | NF-kappa B signaling pathway | 5 | 0.021 | 0.687 |
| map04711 | Circadian rhythm - fly | 3 | 0.024 | 0.715 |
| map00230 | Purine metabolism | 18 | 0.038 | 0.744 |
| map03430 | Mismatch repair | 5 | 0.035 | 0.744 |
| map04111 | Cell cycle - yeast | 10 | 0.033 | 0.744 |
| map04115 | p53 signaling pathway | 6 | 0.037 | 0.744 |
| map04670 | Leukocyte transendothelial migration | 7 | 0.037 | 0.744 |
| map04927 | Cortisol synthesis and secretion | 5 | 0.031 | 0.744 |
| map03410 | Base excision repair | 5 | 0.044 | 0.765 |
| map04022 | cGMP-PKG signaling pathway | 11 | 0.048 | 0.765 |
| map04530 | Tight junction | 12 | 0.043 | 0.765 |

^a Pathways describing human disease not shown

^b Fisher's exact test

^c FDR-corrected

Table S13. Top candidate genes associated with flatwing

| Coordinates | | | | | | |
|---------------------|--------------|-------------|----------------|----------------|--|---------------------------|
| Scaffold | Start | Stop | Gene ID | | Description^a | Source^b |
| Contig10220_pilon | 78887 | 163134 | TOT000182.1 | YGD6 | Zinc-type alcohol dehydrogenase-like protein C1773.06c | Top 1% |
| Contig11287_pilon | 199864 | 215783 | TOT001075.1 | HNF4 | Transcription factor HNF-4 homolog | Top 1% |
| Contig12423_pilon | 12805 | 162659 | TOT001854.1 | OSM3 | Osmotic avoidance abnormal protein 3 | Top 1% |
| Contig12752_pilon | 14326 | 68612 | TOT002129.1 | ROR1 | Inactive tyrosine-protein kinase transmembrane receptor ROR1 | Top 1% |
| Contig12919_pilon | 275064 | 329308 | TOT002239.1 | CLOCK | Circadian locomotor output cycles protein kaput | Top 1% DEG |
| Contig13810_pilon | 43734 | 77412 | TOT002877.1 | CRTAP | Cartilage-associated protein | Top 1% |
| Contig140_pilon | 14528 | 100227 | TOT003072.1 | PP4R1 | Serine/threonine-protein phosphatase 4 regulatory subunit 1 | Top 1% |
| Contig17198_pilon | 217974 | 328434 | TOT004721.1 | SCN60 | Sodium channel protein 60E | Top 1% |
| Contig17198_pilon | 398116 | 526355 | TOT004722.1 | SCN60 | Sodium channel protein 60E | Top 1% |
| Contig17528_pilon | 151965 | 161397 | TOT004867.1 | OBSTE | Protein obstructor-E | Kauai DEG |
| Contig17791_pilon | 294998 | 303418 | TOT005017.1 | PKRA | Protein krasavietz | DEG QTL |
| Contig18506_pilon | 5030 | 106086 | TOT005335.1 | STRN3 | Striatin-3 | Top 1% |
| Contig20777_pilon | 197732 | 433721 | TOT006213.1 | COLL | Transcription factor collier | Top 1% BSA |
| Contig23358_pilon | 266813 | 357642 | TOT006927.1 | E78C | Ecdysone-induced protein 78C (Eip78C) | Top 1% |
| Contig23647_pilon | 61437 | 289082 | TOT006991.1 | RAVR1 | Ribonucleoprotein PTB-binding 1 | Top 1% |
| Contig24519_pilon | 221508 | 332371 | TOT007217.1 | A0A167 WTZ1 | Endo-1,3(4)-beta-glucanase | Top 1% |
| Contig24519_pilon | 569981 | 635619 | TOT007221.1 | SEPIA | Pyrimidodiazepine synthase | Top 1% |
| Contig30320_pilon | 33122 | 79411 | TOT008755.1 | PTPC1 | Protein tyrosine phosphatase domain-containing protein 1 | Top 1% |
| Contig3077_pilon | 487713 | 492969 | TOT008894.1 | REXO4 | RNA exonuclease 4 | Top 1% |
| Contig31374_pilon | 378769 | 413960 | TOT009065.1 | CPT2 | Carnitine O-palmitoyltransferase 2, mitochondrial | Top 1% |
| Contig31374_pilon | 461061 | 489320 | TOT009067.1 | FRM4B | FERM domain-containing protein 4B | Top 1% |
| Contig32190_pilon | 94344 | 248306 | TOT009274.1 | RN207 | RING finger protein 207 | Top 1% |
| Contig35402_pilon | 14084 | 125884 | TOT010060.1 | ABCG1 | ATP-binding cassette sub-family G member 1 | Top 1% |
| Contig37346_pilon.1 | 133394 | 180067 | TOT010542.1 | SCYL1 | N-terminal kinase-like protein | Top 1% |
| Contig40107_pilon | 150347 | 172207 | TOT011176.1 | THUM3 | THUMP domain-containing protein 3 | DEG, QTL |
| Contig4430_pilon | 60074 | 108676 | TOT012009.1 | LAR | Tyrosine-protein phosphatase Lar | Top 1% |
| Contig4497_pilon | 323 | 114981 | TOT012126.1 | MYO5A | Unconventional myosin-Va | Top 1% |

| | | | | | | |
|-------------------|--------|--------|-------------|----------------|---|---------------|
| Contig48084_pilon | 4534 | 15580 | TOT012711.1 | KPEL | Serine/threonine-protein kinase pelle | Top 1% |
| Contig48322_pilon | 73569 | 78934 | TOT012764.1 | CAH10 | Carbonic anhydrase-related protein 10 | Top 1% |
| Contig52923_pilon | 4299 | 134158 | TOT013504.1 | RENT2 | Regulator of nonsense transcripts 2 | Top 1% DEG |
| Contig52923_pilon | 172817 | 234071 | TOT013505.1 | NBL1 | Neuroblastoma suppressor of tumorigenicity 1 | Top 1% |
| Contig53931_pilon | 135337 | 200203 | TOT013689.1 | TADBP | TAR DNA-binding protein 43 | Top 1% |
| Contig55532_pilon | 2641 | 6823 | TOT013967.1 | SOSSC | SOSSC_BOVIN | Top 1% |
| Contig5817_pilon | 13001 | 94458 | TOTO14395.1 | A0A1B6 LWD6 | Uncharacterized protein | Top 1% |
| Contig6025_pilon | 181847 | 338853 | TOT014693.1 | PAX6 | Paired box protein Pax-6 | Top 1% |
| Contig6181_pilon | 7490 | 15461 | TOT014894.1 | MYCT | Proton myo-inositol cotransporter | Top 1% |
| Contig6371_pilon | 72321 | 126646 | TOT015146.5 | GOGA4 | Golgin subfamily A member 4 | Top 1% |
| Contig6636_pilon | 248427 | 279756 | TOT015511.1 | A0A067 RPQ2 | LRR domain-containing protein | Top 1% |
| Contig6636_pilon | 332473 | 344815 | TOT015512.1 | IPR0110 11 | Uncharacterized protein | Top 1% |
| Contig66512_pilon | 19778 | 188429 | TOT015537.1 | LASP1 | LIM and SH3 domain protein F42H10.3 | Top 1% DEG |
| Contig6932_pilon | 94582 | 114944 | TOT015868.1 | ABCB8 | ATP-binding cassette sub-family B member 8, mitochondrial | Top 1% |
| Contig6932_pilon | 132941 | 150338 | TOT015869.1 | APMAP | Adipocyte plasma membrane-associated protein | Top 1% |
| Contig7020_pilon | 57223 | 96643 | TOT015999.1 | SPS1 | Selenide, water dikinase | Top 1% |
| Contig7210_pilon | 172512 | 326460 | TOT016305.1 | MYO | myoglianin | Top 1% |
| Contig7490_pilon | 12720 | 16839 | TOT016652.1 | GCN5 | Histone acetyltransferase GCN5 | Top 1% |
| Contig8190_pilon | 192630 | 256540 | TOT017431.1 | AT133 | Probable cation-transporting ATPase 13A3 | Top 1% |
| Contig82459_pilon | 106133 | 176987 | TOT017512.1 | UNC89 | Muscle M-line assembly protein unc-89 | DEG QTL |
| Contig83863_pilon | 1777 | 51856 | TOT017662.1 | A0A017 RSC4 | Uncharacterized protein | Top 1% |
| Contig92683_pilon | 43257 | 76189 | TOT018508.1 | A0A0T6 B8G7 | Uncharacterized protein | Top 1% |
| Contig33215_pilon | 67326 | 419738 | TOT009518.1 | PLXA4 | Plexin-A4 | QTL BSA |
| Contig43580_pilon | 106377 | 137341 | TOT011864.1 | RNF41 | E3 ubiquitin-protein ligase NRDP1 | QTL BSA |

^a Functional descriptions and references provided in Main Text

^b The criterion for inclusion as a top candidate was that a gene had to receive support for association with the flatwing phenotype from at least two of the following four sources:

QTL = portion of the gene was located within a 1 kb flanking region of a significantly-associated (FDR-corrected) marker in the flatwing QTL analysis

Top1% = portion of the gene was located within a 1 kb flanking region of a SNP in the top 1% of significantly-associated markers in the flatwing QTL analysis (Top1% candidates automatically received “QTL” support)

BSA = portion of the gene was located within a 1 kb flanking region of a significantly-associated marker from the previously-published bulked segregant analysis of Kauai flatwing males⁷ which was also anchored to LG1

DEG = gene was significantly differentially expressed between pure-breeding *normal-wing* genotypes and *flatwing* genotypes, in embryonic thoracic tissue (track iv of Fig. 2a in Main Text)

Table S14. GO analysis of candidate flatwing-associated genes (CGs)

| GO | Type | Function | No. of CGs | <i>P</i> -adj. (χ^2 test) |
|------------|--------------------|---|------------|---------------------------------|
| GO:0010720 | biological_process | positive regulation of cell development | 3 | <0.001 |
| GO:0045597 | biological_process | positive regulation of cell differentiation | 3 | 0.002 |
| GO:0060284 | biological_process | regulation of cell development | 3 | 0.042 |
| GO:0003707 | molecular_function | steroid hormone receptor activity | 2 | <0.001 |
| GO:0009755 | biological_process | hormone-mediated signaling pathway | 2 | 0.006 |
| GO:0030545 | molecular_function | receptor regulator activity | 2 | 0.035 |
| GO:0043401 | biological_process | steroid hormone mediated signaling pathway | 2 | 0.002 |
| GO:0045666 | biological_process | positive regulation of neuron differentiation | 2 | 0.040 |
| GO:0048018 | molecular_function | receptor ligand activity | 2 | 0.022 |

Table S15. Principal components with eigenvalues > 1 from PCA on male CHC profiles. MANOVA^a results examine the effect of male morph on scores for each PC (multivariate model: Wilks' $\lambda = 0.517$, $F_{6,191} = 29.769$, $p < 0.001$)

| Principal component | Eigenvalue | % Variance explained | F _{1,196} | P | R ² |
|---------------------|------------|----------------------|--------------------|--------|----------------|
| 1 | 9.408 | 36.18 | 25.885 | <0.001 | 0.131 |
| 2 | 2.635 | 10.136 | 18.040 | <0.001 | 0.092 |
| 3 | 2.490 | 9.576 | 21.454 | <0.001 | 0.109 |
| 4 | 1.888 | 7.261 | 0.001 | 0.979 | 0.000 |
| 5 | 1.315 | 5.058 | 25.741 | <0.001 | 0.131 |
| 6 | 1.020 | 3.925 | 4.079 | 0.043 | 0.021 |

^a Two-sided tests

Table S16. Candidate gene set associated with each CHC phenotype (individual or principal component) that yielded a significant QTL on the putative X (LG1), with the flatwing QTL for comparison

| Coordinates | | | Gene ID | Trait | | | | | | | | | | | | Flat-wing | Description |
|---------------------|--------|--------|-------------|----------------------|---|---|---|----|----|-----|----|---|---|---|---|------------|--|
| Scaffold | Start | Stop | | Individual Compounds | | | | | | PCs | | | | | | | |
| | | | 1 | 5 | 7 | 8 | 9 | 12 | 15 | 18 | 21 | 1 | 4 | 6 | | | |
| Contig10220_pilon | 78887 | 163134 | TOT000182.1 | √ | √ | √ | √ | | | √ | √ | √ | √ | √ | √ | YGD6 | Zinc-type alcohol dehydrogenase-like protein C1773.06c |
| Contig11287_pilon | 199864 | 215783 | TOT001075.1 | √ | √ | √ | √ | √ | √ | √ | √ | √ | √ | √ | √ | HNF4 | Transcription factor HNF-4 homolog |
| Contig12423_pilon | 12805 | 162659 | TOT001854.1 | √ | √ | √ | √ | √ | √ | √ | √ | √ | √ | √ | √ | OSM3 | Osmotic avoidance abnormal protein 3 |
| Contig14561_pilon | 436209 | 450946 | TOT003337.1 | | | | | | | √ | | | | | | CAS | Transcription factor castor |
| Contig16800_pilon | 571706 | 708271 | TOT004499.1 | | | | | | | √ | | | | | | SMAD3 | Mothers against decapentaplegic homolog 3 |
| Contig17198_pilon | 217974 | 328434 | TOT004721.1 | | √ | | | | | | | | | √ | √ | SCN60 | Sodium channel protein 60E |
| Contig17198_pilon | 398116 | 526355 | TOT004722.1 | √ | | | √ | | | √ | | √ | | √ | | SCN60 | Sodium channel protein 60E |
| Contig17589_pilon | 46372 | 264973 | TOT004897.1 | | | | | | √ | √ | | | | | | SSBP3 | Single-stranded DNA-binding protein 3 |
| Contig17589_pilon | 70840 | 324258 | TOT004898.1 | | | | | | √ | √ | | | | | | ATG10 | Ubiquitin-like-conjugating enzyme ATG10 |
| Contig17791_pilon | 294998 | 303418 | TOT005017.1 | √ | √ | | | | | √ | √ | | | | √ | PKRA | Protein krasavietz |
| Contig18309_pilon | 75967 | 136785 | TOT005266.1 | | √ | | | | | | | | | | | STA5B | Signal transducer and activator of transcription 5B |
| Contig191692_pilon | 10444 | 19353 | TOT005602.1 | | | | | | | √ | | | | | | GNAI | Guanine nucleotide-binding protein G(i) subunit alpha |
| Contig20777_pilon | 197732 | 433721 | TOT006213.1 | √ | √ | | | | √ | √ | √ | √ | √ | | √ | COLL | Transcription factor collier |
| Contig23454_pilon | 18213 | 89940 | TOT006946.1 | | √ | | | | | √ | | | | | | ARD17 | Arrestin domain-containing protein 17 |
| Contig23647_pilon | 61437 | 289082 | TOT006991.1 | √ | √ | √ | √ | | | √ | √ | √ | √ | √ | √ | RAVR1 | Ribonucleoprotein PTB-binding 1 |
| Contig24519_pilon | 569981 | 635619 | TOT007221.1 | | | | | | | √ | | | | | √ | SEPIA | Pyrimidodiazepine synthase |
| Contig27628_pilon | 259968 | 507152 | TOT008051.1 | | | | | | | √ | | | | | | PROH3 | Prohormone-3 |
| Contig29117_pilon | 70169 | 396634 | TOT008443.1 | | √ | √ | √ | | | √ | | | | | | CCKAR | Cholecystokinin receptor type A |
| Contig29877_pilon | 36855 | 181557 | TOT008655.1 | | √ | | | | | | | | | | | E41LA | Band 4.1-like protein 4A |
| Contig3077_pilon | 487713 | 492969 | TOT008894.1 | √ | √ | √ | √ | √ | √ | √ | √ | √ | √ | √ | √ | REXO4 | RNA exonuclease 4 |
| Contig3077_pilon | 528735 | 564924 | TOT008896.1 | | √ | | | | | | | | | | | P4K2B | Phosphatidylinositol 4-kinase type 2 |
| Contig31374_pilon | 461061 | 489320 | TOT009067.1 | √ | √ | √ | √ | √ | √ | √ | √ | √ | √ | √ | √ | FRM4B | FERM domain-containing protein 4B |
| Contig32190_pilon | 94344 | 248306 | TOT009274.1 | √ | √ | √ | √ | | | √ | √ | √ | √ | √ | √ | RN207 | RING finger protein 207 |
| Contig3429_pilon | 122631 | 136033 | TOT009790.1 | √ | | | | | | √ | | | | | | A0A1B6JV12 | Uncharacterized protein |
| Contig3536_pilon | 221796 | 347378 | TOT010046.1 | | √ | | | | | √ | | | | | | GNAO | Guanine nucleotide-binding protein G(o) subunit alpha |
| Contig35402_pilon | 14084 | 125884 | TOT010060.1 | | √ | √ | | | | √ | | √ | √ | √ | | ABCG1 | ATP-binding cassette sub-family G member 1 |
| Contig3552_pilon | 175659 | 203623 | TOT010094.1 | | √ | | | | | √ | | | | | | OSBL9 | Oxysterol-binding protein-related protein 9 |
| Contig37346_pilon.1 | 133394 | 180067 | TOT010542.1 | √ | √ | √ | √ | √ | √ | √ | √ | √ | √ | √ | √ | SCYL1 | N-terminal kinase-like protein |
| Contig40569_pilon | 70324 | 81832 | TOT011293.1 | √ | | | | | | √ | | | | | | NXT1 | NTF2-related export protein |
| Contig43774_pilon | 63974 | 228355 | TOT011905.1 | | | | | | | √ | | | | | | HMCN1 | Hemicentin-1 |
| Contig4430_pilon | 60074 | 108676 | TOT012009.1 | √ | √ | √ | | | √ | √ | √ | √ | | √ | | LAR | Tyrosine-protein phosphatase Lar |
| Contig4451_pilon | 20121 | 45182 | TOT012039.1 | | √ | | | | | | | | | | | LAR4 | La-related protein Larp4B |
| Contig48084_pilon | 4534 | 15580 | TOT012711.1 | | √ | | | | | √ | | | | | √ | KPEL | Serine/threonine-protein kinase pelle |
| Contig48322_pilon | 73569 | 78934 | TOT012764.1 | | | | | | | √ | | | | | √ | CAH10 | Carbonic anhydrase-related protein 10 |
| Contig5051_pilon | 34769 | 44241 | TOT013154.1 | | | | | | | √ | | | | | | CMYA5 | Cardiomyopathy-associated protein 5 |
| Contig52923_pilon | 172817 | 234071 | TOT013505.1 | √ | √ | √ | √ | | √ | √ | √ | √ | √ | √ | √ | NBL1 | Neuroblastoma suppressor of tumorigenicity 1 |

| | | | | | | | | | | | | | | |
|-------------------|--------|--------|-------------|---|---|---|---|---|---|---|---|---|------------|---|
| Contig53931_pilon | 135337 | 200203 | TOT013689.1 | √ | √ | √ | | √ | √ | √ | √ | √ | TADBP | TAR DNA-binding protein 43 |
| Contig5490_pilon | 190540 | 238169 | TOT013863.1 | | √ | | | | √ | | | | UNC89 | Muscle M-line assembly protein unc-89 |
| Contig5490_pilon | 145320 | 153034 | TOT013873.1 | | | | | | √ | | | | A0A067RCZ8 | Uncharacterized protein |
| Contig5542_pilon | 24715 | 684526 | TOT013934.1 | | √ | | | | √ | | | | GALT2 | Polypeptide N-acetylgalactosaminyltransferase 2 |
| Contig55532_pilon | 2641 | 6823 | TOT013967.1 | | √ | | | | √ | | | | SOSSC | SOSS complex subunit C |
| Contig5817_pilon | 13001 | 94458 | TOT014395.1 | | | √ | | | √ | | | | A0A1B6LWD6 | Uncharacterized protein |
| Contig6025_pilon | 181847 | 338853 | TOT014693.1 | √ | √ | √ | √ | | √ | √ | √ | √ | PAX6 | Paired box protein Pax-6 |
| Contig6181_pilon | 7490 | 15461 | TOT014894.1 | | √ | | | | √ | | √ | √ | MYCT | Proton myo-inositol cotransporter |
| Contig6371_pilon | 72321 | 126646 | TOT015146.5 | √ | √ | √ | | √ | √ | √ | √ | √ | GOGA4 | Golgin subfamily A member 4 |
| Contig63833_pilon | 68993 | 231055 | TOT015158.1 | | | | | | √ | | | | HUWE1 | E3 ubiquitin-protein ligase HUWE1 |
| Contig6636_pilon | 248427 | 279756 | TOT015511.1 | √ | √ | √ | | √ | √ | √ | √ | √ | A0A067RPQ2 | LRR domain-containing protein |
| Contig66512_pilon | 19778 | 188429 | TOT015537.1 | √ | √ | | | √ | √ | √ | √ | √ | LASP1 | LIM and SH3 domain protein F42H10.3 |
| Contig6932_pilon | 94582 | 114944 | TOT015868.1 | | √ | | | | √ | | | | ABCB8 | ATP-binding cassette sub-family B member 8, mitochondrial |
| Contig6932_pilon | 132941 | 150338 | TOT015869.1 | | √ | | | | √ | | | √ | APMAP | Adipocyte plasma membrane-associated protein |
| Contig7210_pilon | 172512 | 326460 | TOT016305.1 | √ | √ | √ | | √ | √ | √ | √ | √ | MYO | myoglianin |
| Contig745_pilon | 6060 | 59826 | TOT016600.1 | | | | | | √ | | | | E41L5 | Band 4.1-like protein 5 |
| Contig7490_pilon | 12720 | 16839 | TOT016652.1 | √ | √ | √ | | √ | √ | √ | √ | √ | GCN5 | Histone acetyltransferase GCN5 |
| Contig8263_pilon | 12087 | 12734 | TOT017545.1 | | √ | √ | | | √ | | √ | √ | TWF | Twinfilin |
| Contig92683_pilon | 43257 | 76189 | TOT018508.1 | √ | √ | √ | √ | √ | √ | √ | √ | √ | A0A0T6B8G7 | Uncharacterized protein |

30

